Low Temperature Physics/Fizika Nizkikh Temperatur, 2017, v. 43, No. 8, pp. 1207–1213

Single crystals growth of hexaferrits M-type $MTi_xCo_xFe_{12-2x}O_{19}$ (M = Ba, Sr) by floating zone and investigation of their magnetic and magnetoelectric properties

A.M. Balbashov[1], M.E. Voronchikhina[1], L.D. Iskhakova[2], V.Yu. Ivanov[3], and A.A. Mukhin[3]

[1]*Moscow Power Engineering Institute, Moscow, Russia*
E-mail: BalbashovAM@mpei.ru

[2]*Fiber Optics Research Center of RAS, Moscow, Russia*

[3]*Prokhorov General Physics Institute of RAS, Moscow, Russia*

Received January 2, 2017, published online June 26, 2017

Floating zone melting method with optical heating is elaborated to grow single crystals of the substituted hexaferrites $BaTi_xCo_xFe_{12-2x}O_{19}$ and $Sr_xTi_xCo_xFe_{12-2x}O_{19}$ ($0.8 \le x \le 2$). The dynamics of the growth process is studied and results of the analysis of impurity phases appearing in the initial stages of the crystal growth are presented. Compositions and unit-cell parameters of crystals are determined. Electrical, magnetic and magnetoelectric properties of grown crystals are investigated at temperatures 2–365 K and magnetic fields up to 50 kOe. It is shown that the resistivity of annealed in oxygen crystals at room temperature is ~ 10^6 Ohm·cm while at helium temperatures the crystals become good insulators. Magnetic measurements reveal conical spin structures in the crystals at some concentrations and temperatures. Magnetic field induced electric polarization of the low value (~ 0.3 μC/m^2) is detected at liquid helium temperatures for compositions with Ti and Co concentrations x = 0.8–0.9.

PACS: 75.47.Np Metals and alloys;
75.50.–y Studies of specific magnetic materials;
7**5.85.+t** Magnetoelectric effects, multiferroics.

Keywords: magnetic and magnetoelectric properties, hexaferrits, crystals growth, floating zone melting.

1. Introduction

Hexaferrites are ferrimagnetic materials with hexagonal structure which are actively studied as a promising material with wide applications: permanent magnets, devices for recording and storage of information, components of various electronic devices [1]. Among them a significant attention is attracted to barium and strontium hexaferrites of M-type as well as their substituted compositions, for example, $Ba_xTi_xCo_xFe_{12-2x}O_{19}$ (x = 0–6) which possess a high magnetization, and controllable magnetic anisotropy at room temperature. A new impetus to their study aroused in recent years with the discovery of multiferroelectricity in number of Y, Z and M-type hexaferrites including relatively high (up to room) temperatures [2–4]. Usually polycrystalline samples have been used for practical applications and physical studies; these compounds were obtained by hydrothermal synthesis, sol-gel technology (see, e.g., [1,5–7]). Recently, an interest to the hexaferrite producing in the form of nanomaterials or oriented films has grown [8,9]. Only a small number of papers are devoted to the study of single crystalline multiferroic hexaferrites. Obviously, researches on single crystals allow to perform more detailed study of physical mechanisms of magnetoelectric phenomena and to obtain the maximum of magnetoelectric coupling as well as to clarify the effects of magneto-crystalline anisotropy in these processes.

Growth of high quality single crystals of hexaferrites is a rather difficult task. There were enough successful attempts of the growth of the $BaFe_{12-x-0.05}Sc_xMg_{0.05}O_{19}$ crystals by floating zone melting [10]. The Ref. 11 describes the growth of samarium-activated single crystals of the $SrFe_{12}O_{19}$ in the form of hexagonal plates with dimensions of 10 mm in length and 3–4 mm width by spontaneous crystallization from the melt. Single crystals of Ti-substituted barium hexaferrite $BaFe_{12-x}Ti_xO_{19}$ with x up to 1.3

and sizes 2–8 mm were grown by spontaneous crystallization from molten sodium carbonate flux [12]. The difficulty of single crystal growth of substituted hexaferrites M-type is due to an incongruent nature of melting. A phase diagram of the $BaO–Fe_2O_3$ system was studied only partially, but nevertheless it allows to make a conclusion on a nature of the incongruent melting of BaM–ferrite [1]. According to Ref. 13, where an iron oxide-rich region of the $SrFe_{12}O_{19}$ crystallization is studied, the hexaferrite remains stable up to 1410 °C and decomposes at higher temperatures with a formation of W- and X-hexaferrites. The Ref. 14 on the examples of growth of the $MFe_{12}O_{19}$ (M = Sr, Ba) crystals shows that the degree of incongruent melting is affected by increasing of partial pressure above the melt, and a congruent melting can be achieved at a pressure above 100 atm. Furthermore, at low partial oxygen pressure the Fe^{3+} ions transform partly to Fe^{2+} ones resulting thus in a significant increase of electrical conductivity.

The aim of this work was to grow high quality bulk single crystals of substituted hexaferrites $SrTi_xCo_xFe_{12-2x}O_{19}$ and $BaTi_xCo_xFe_{12-2x}O_{19}$ and study their electrical and magnetic properties. Our interest in the study of hexaferrites is determined by the search for new compounds possessing multiferroelectric properties. The conventional mechanism of electric polarization in hexaferrite M- [10], Y- [2,15] and Z-types [3,4] is the mechanism of the spin current (or inverse Dzyaloshinskii–Moriya interaction) [16,17], which is manifested in transverse conical spin structures including magnetic field induced ones. Such structures and associated multiferroelectric properties were observed in the substituted system $BaSc_xFe_{12-x}O_{19}$ [10,21]. The conical magnetic structure obtained by neutron diffraction was discovered in another M-type substituted system: $BaTi_xCo_xFe_{12-2x}O_{19}$ [18,19]. Some magnetic and electric properties of one single crystal from this series were investigated recently [22,23]

2. Experimental

The growth of the $SrTi_xCo_xFe_{12-2x}O_{19}$ and $BaTi_xCo_xFe_{12-2x}O_{19}$ crystals was carried out by floating-zone melting method with radiation heating using the zone melting apparatus URN-2-ZM, equipped with the crystallization chamber of the high pressure, allowing to carry out the processes of growth under oxygen pressure up to 100 atm, and possessing a high-temperature annealing of the grown crystals [14].

Polycrystalline feed rods with a diameter of 7 mm, were made by usual ceramic technology using high purity Fe_2O_3, CoO, $BaCO_3$, $SrCO_3$, TiO_2. Crystal growth was performed with a rate of 5–10 mm/h; the oxygen pressure in the chamber was 60–70 atm; the rotation of the crystal and the seed were 40 rpm and 1 rpm, respectively. The grown crystals were obtained as cylinders with a diameter ~ 6 mm and a length ~ 60 mm.

The characterization of the samples was performed by diffraction methods (x-ray phase analysis and Laue method). Microstructure of the samples was investigated using JSM-5910LV (JEOL) scanning electron microscope in Z-contrast back-scattered electrons mode. Determination of the chemical composition was carried out by means of x-ray energy dispersive analysis using AZtecENERGY (Oxford Instruments) analytical system. Single crystals of TiO_2, $CoGa_2O_4$, $SrFe_{12}O_{19}$ and $BaFe_{12}O_{19}$ were used as standards/references for the calculation of the chemical element composition. The x-ray analysis (XRD) of the samples was performed using Bruker D2 Phaser powder x-ray diffractometer with Cu-K_α radiation. Processing of the results and the phase analysis of samples was accomplished by software packages DIFFRAC^{plus} (EVA and TOPAS 4.2.0.2). The orientation of the samples with respect to the crystallographic axes was performed by the x-ray Laue using digital apparatus of photonic science.

For measurements of electric and magnetoelectric properties of crystals plane-parallel samples were cut in a form of disks or rectangular plates with a thickness 0.8–1.5 mm and an area 10–30 mm^2. Usually the measurements were carried out of samples with a hexagonal axis lying in the plane of the plate, however, in some cases the axis was oriented perpendicular to the sample plane. Contacts made of conductive silver paste were applied to flat surfaces of a sample. Electrical properties were measured using a Keithley 6517A electrometer.

The magnetization was measured by a vibrating sample magnetometer in fields up to 14 kOe, and a SQUID magnetometer of Quantum Design (MPMS) in fields up to 50 kOe in the temperature range from 2 to 365 K. Measurements were carried out on samples with ~ 2 mm size and a shape closed to cubic. No correction for the demagnetization factor was performed.

3. Experimental results and discussion

3.1. Crystal growth details

When growing single crystals in the system $SrTi_xCo_xFe_{12-2x}O_{19}$ (x = 0.9–2.0) using both mono- or polycrystalline seed no single crystal growth occurs immediately after crystallization starting. In accordance with the phase diagram of the system $SrO–Fe_2O_3$ [13] iron oxide is crystallized from the melt of stoichiometric composition, and a composition of melt is displaced, reaching the hexaferrite crystallization region. This process promotes by the growth performed under high oxygen pressure. Further, the solidification front formed embryos hexaferrite phases, which progress in size, forming a blocky crystal with traces of impurity phases. With further crystallization the growth of the main hexaferrite phase occurs while the phases of other compositions disappear. Usually a single-phase growth of the crystal starts after ~ 15 mm of the grown boule at the crystallization rate of 5 mm/h. Further

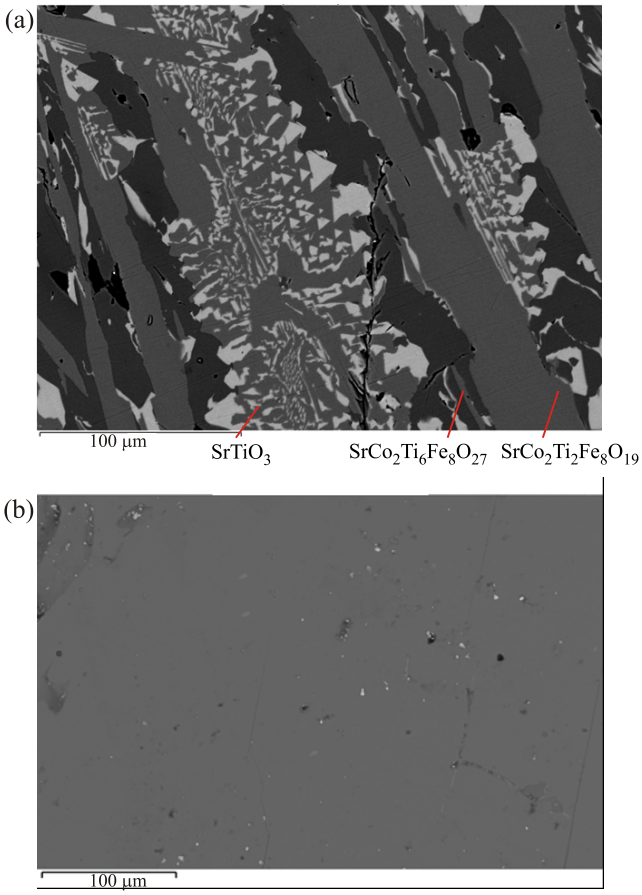

Fig. 1. Microphotography (Z-contrast) of some parts of the cross section of the $SrCo_2Ti_2Fe_8O_{19}$ sample: (a) region corresponding to the initial stages of growth including phases of the $SrTiO_3$ (light enable), $SrCo_2Ti_2Fe_8O_{19}$ (gray region) and $SrCo_2Ti_6Fe_8O_{27}$ (black areas), (b) subsequent grown practically pure $SrCo_2Ti_2Fe_8O_{19}$ phase.

single crystal grows according a mechanism of the competing growth. This process is confirmed by x-ray Laue analysis of grown crystals along the growth axis. Optimal composition of the seed was clarified to provide the growth of single crystals of the substituted M-hexaferrites $MTi_xCo_xFe_{12-2x}O_{19}$. The phase compositions of the two cross sections of the boule of the $SrCo_2Ti_2Fe_8O_{19}$ are mapped in Fig. 1 as an example, where shown are the initial nonequilibrium part of the crystal containing three crystalline phases (a) and single phase-to-phase of the nominal composition $SrCo_2Ti_2Fe_8O_{19}$ (b). As can be seen from Fig. 1(a) it was found in the initial (not single phase) part of the crystal the main M-hexaferrite $SrCo_2Ti_2Fe_8O_{19}$ phase, $SrTiO_3$ phase and $SrCo_2Ti_6Fe_8O_{27}$ unknown phase. The later Sr–Ti–Co enriched phases were not identified by x ray due to its low content in the single crystal and contained mainly in floating zone melt. Thus, for the implementation of the process of single crystal growth using a single crystalline seed it is necessary to modify the initial part of the supplying feed rod end by non-stoichiometric composition with low content of iron oxide. It is well known process of "moved solution crystal growth" (MSCG), where as a solvent components of composition are used. At MSCG the crystal growth speed should be decreased essentially.

During growth of the $BaCo_xTi_xFe_{12-2x}O_{19}$ (x = 0.8–1.1) single crystals the crystallization occurs by a similar manner as for the Sr-hexaferrite. But unlike to the Sr compounds in the Ba ones the formation of only single impurity phase with the $BaFe_2O_4$ structure has been observed (in the single crystalline sample with x = 0.9). According to the review [1], the hexagonal $BaFe_2O_4$ were often observed as an impurity phase for various methods of synthesis of M-type hexaferrites, particularly at temperatures below 1000 °C.

The results of the composition analysis of the Co and Ti substituted various hexaferrites found in their single-phase part of crystals as well as the refined unit-cell parameters of compounds (space group *P*63/*mmc*) are presented in Table. 1. As can be seen from Table 1 the found compositions are closed to the as grown nominal compositions. Some their differences could be attributable to a small content of impurity phases due to large crystallization speed in this MSCG processing.

Table 1. The cationic composition of the substituted single crystals and their unit-cell parameters

Nominal composition	Found cationic composition, at.%			Unit-cell parameters		
	Fe	Co	Ti	a, Å	c, Å	V, Å^3
$BaCo_{0.9}Ti_{0.9}Fe_{10.2}O_{19}$	10.17	1.00	0.90	5.8946(6)	23.237(2)	699.21
$BaCo_{1.1}Ti_{1.1}Fe_{9.8}O_{19}$	10.01	0,96	1.03	5.8943(7)	23.254 (3)	699.64
$SrCo_{1.25}Ti_{1.25}Fe_{9.5}O_{19}$	9.9	0.99	1.1	5.8835(4)	23.085	692.02
$SrCo_{1.5}Ti_{1.5}Fe_9O_{19}$	9.03	1.47	1.45	5.8839(3)	23.086(3)	692.14
$SrCo_{1.75}Ti_{1.75}Fe_{8.5}O_{19}$	8.36	1.84	1.81	5.884(1)	23.097(3)	692.50
$SrCo_2Ti_2Fe_8O_{19}$	8.0	2.02	1.99	5.886(3)	23.112(1)	693.41

The compositions were determined with an accuracy of ±0.06.

3.2. Electrical properties

The room temperature resistivity of grown crystals in the surface layers exceeds 10^7 Ohm·cm, but at cleaves it is equal ~ 10^4–10^6 Ohm·cm. After annealing of the single crystalline plates of 5×5×1 mm size at temperatures of 600–800 °C the resistance at the surface was increased above 10^9 Ohm·cm, but at cleaves it was not exceed 10^6 Ohm·cm, i.e., the resistance is increased only in a fairly thin (few micrometers) surface layer, indicating a small oxygen diffusion into the crystal. Such resistance is not enough for the magnetoelectric measurements at room temperature. Besides, it turned out that the current-voltage characteristics are highly nonlinear, namely, the resistance significantly decreases with the increase of applied voltage. As temperature decreases, the resistance increases approximately exponentially (Fig. 2). At liquid nitrogen temperatures the resistance becomes ~ 10^{10}–10^{13} Ohm·cm, whose value already suitable for pyroelectric measurements in the absence of applied voltage. However, at voltage of ~ 100 V a relatively noticeable current will leak in addition to possible pyroelectric currents. Finally, at helium temperatures, the samples are almost perfect insulators, and voltage of several hundred Volts is not cause the ohmic currents capable for measurements.

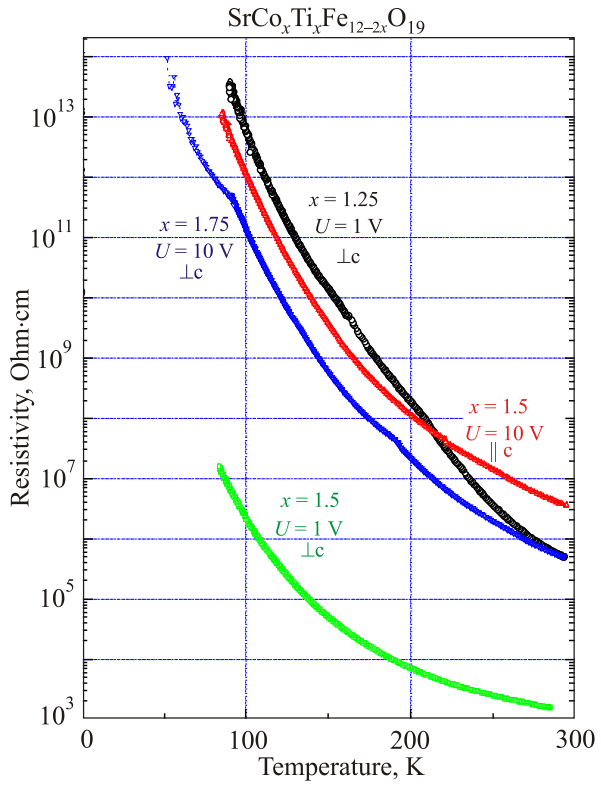

Fig. 2. (Color online) The temperature dependences of electrical resistivity of some SrCo$_x$Ti$_x$Fe$_{12-2x}$O$_{19}$ crystals measured at applied voltage of 1 or 10 V. All curves were obtained for the annealed samples, while the green curve obtained for not annealed ones.

3.3. Magnetic properties

The results of measurements of magnetization in barium hexaferrites BaTi$_x$Co$_x$Fe$_{12-2x}$O$_{19}$ (x = 0.8, 0.9, and 1.1) are in a reasonable agreement with known previously data cited in the literature, for example, for single crystals at room temperature [19] or polycrystals at liquid helium [20]. Some quantitative differences could be due to different technologies of their obtaining and, consequently, some differences between the real and nominal compositions (see Fig. 3). In particular, crystals with x = 0.8 have a clear uniaxial anisotropic character with easy direction along c axis. When x = 0.9 the anisotropy is slightly reduced, and at low temperatures after reaching the saturation magnetization perpendicular to the c axis becomes higher than along it. Crystals with x = 1.1 have the intermediate anisotropy from the easy axis to the easy plane. At room temperature and in weak fields at low temperatures, they are still easier magnetized along c axis, but at the field ~ 7 kOe, the magnetization perpendicular to the c axis increases sharply at low temperatures and exceeds the magnetization along the c axis. According to Ref. 19 the hexaferrite with x = = 1.1 behaves already like easy plane one at the room temperature. It should also be noted that during the initial magnetization in the basal plane saturation is achieved in stronger fields than in subsequent cycles. The Fig. 3 also shows decrease of saturation of magnetization with increasing x.

As already mentioned, neutron diffraction data indicate the existence of the conical spin structures at low temperatures for the compositions with x = 0.8 and 1.1 [19]. Our magnetic data also suggest the presence of such structures, at least for the compositions with x = 0.9 and 1.1. This conclusion is supported by the presence of maximum in the temperature dependences of the magnetization measured at fixed fields (~ 280 K for x = 1.1 and ~ 170 K for x = 0.9). However, temperatures at which the maxima occur depend on the values of the field, and very slightly manifested in measurements along the c axis. The existence of conical structures is also confirmed by different slopes of the magnetization curves at liquid helium and room temperatures (Fig. 3). In the case of x = 0.8 the slope of the curves at 5 and 295 K are approximately equal, and the maximum in the temperature dependence of the magnetization almost is not seen. Therefore, if the conical structure occurs for this composition, its cone angle is quite small, so the transition to the conical structure is not manifested significantly in the magnetic properties.

Let us consider the magnetic properties of an isostructural system SrTi$_x$Co$_x$Fe$_{12-2x}$O$_{19}$, whose systematic researches are still not carried out so far, especially for single crystals. Magnetization curves at room temperature measured along and perpendicular to hexagonal c axis for crystals with x = 1.25, 1.5, 1.75 and 2.0 are shown in Figs. 4(a)–(d). As can be seen,

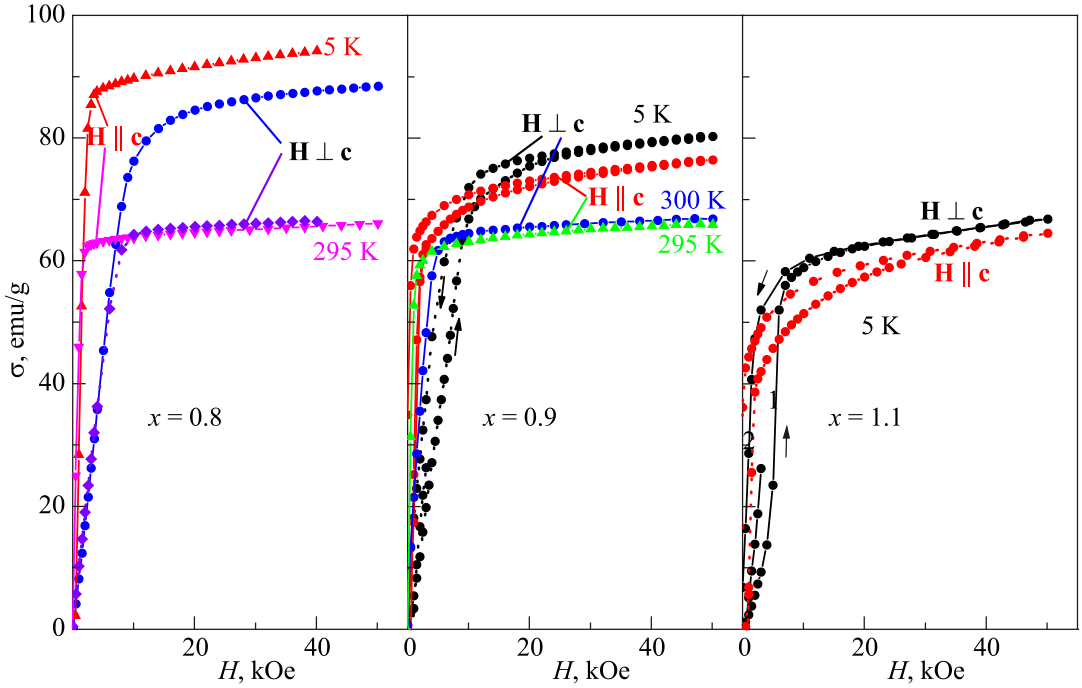

Fig. 3. (Color online) The magnetization curves of the $BaCo_xTi_xFe_{12-2x}O_{19}$ crystals of different compositions at liquid helium and room temperatures.

the character of the magnetic anisotropy is changed from the easy axis (x = 1.25) to the easy plane ($x \geq 1.75$) with increasing of concentration x. The concentration x = 1.5 exhibits an intermediate character: in weak magnetic fields the susceptibility along the c axis is large, however, the magnetization in the basis plane exceeds the magnetization along the c axis in sufficiently high fields, i.e., the change of the anisotropy in the Sr hexaferrite is similar to that observed in the $BaTi_xCo_xFe_{12-2x}O_{19}$ system near x = 1.1. Figure 4 clearly shows the reduction of the magnetization saturation upon the substitution of Fe to Co and Ti.

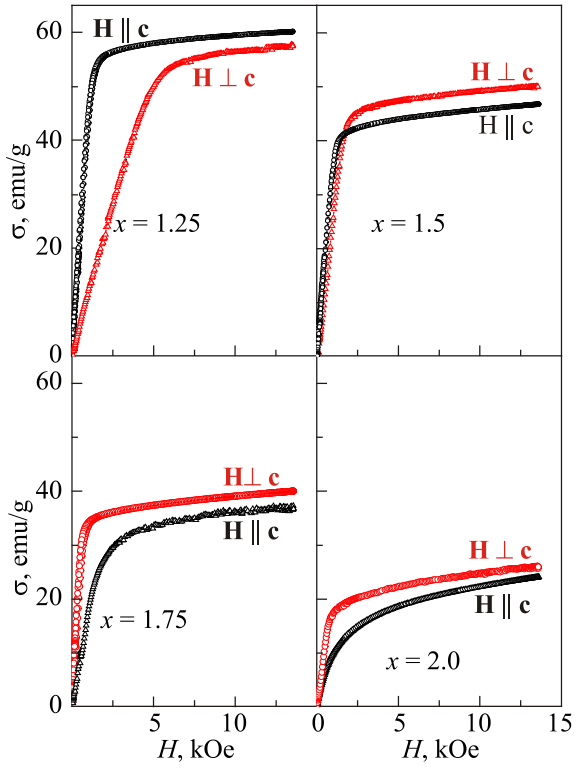

Fig. 4. The magnetization curves of the $SrCo_xTi_xFe_{12-2x}O_{19}$ crystals (x = 1.25, 1.5, 1.75 and 2.0) at the room temperature.

At low temperatures (Fig. 5) the magnetization curves are more complicated: there is a noticeable hysteresis, and the curve at the first cycle of magnetization in the basal plane differs noticeably from the curves for subsequent cycles, especially in the easy plane crystals. The latter could be explained by the fact that in the demagnetized state of easy plane crystals there are ferromagnetic domains oriented at various directions in the basis plane and their alignment along the magnetic field requires more efforts than a change of resulting magnetization for 180° of the already magnetized crystal. We note also the possible formation of conical structures at low temperatures for the compositions with $x < 1.5$ similar to substituted $BaCo_xTi_xFe_{12-2x}O_{19}$ [19] and $BaSc_xFe_{12x}O_{19}$ [10] systems, that is evidenced by the maxima in the temperature dependence of the susceptibility along and perpendicular to the c axis as well as decreasing in the magnetization curves slope when the temperature goes up from helium to room ones. However, as in the case of the $BaCo_xTi_xFe_{12-2x}O_{19}$, system these effects are too weak compare with the $BaSc_xFe_{12x}O_{19}$ [21], and only magnetic measurements are not enough to conclude unambiguously about the existence of the conical structure in the $SrCo_xTi_xFe_{12-2x}O_{19}$ system.

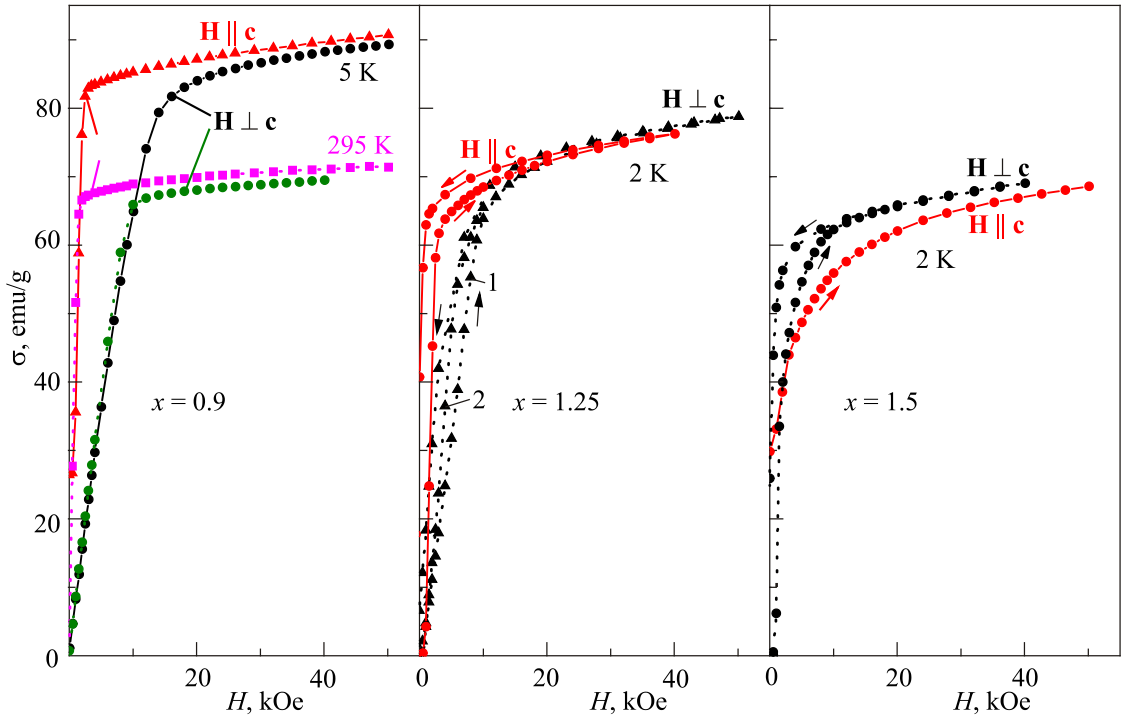

Fig. 5. The magnetization curves of the $SrCo_xTi_xFe_{12-2x}O_{19}$ crystals (x = 0.9, 1.25 and 1.5) at helium temperatures.

3.4. Magnetoelectric properties

We have tried to detect the electric polarization induced by the joint action of electric and magnetic fields. According to the results of previous sections it follows immediately that at room temperature this is impossible due to high conductivity. At nitrogen temperature (77.3 K) no change pyrocurrent was observed with the magnetic field (only a slow monotonic drift due to a discharge of the effective capacitance after turning off the voltage was observed).

However, at helium temperatures in crystals with the smallest x in the classical geometry (**P** ⊥ **H** ⊥ **c**) and after preliminary cooling down in electric and magnetic fields (poling) we were able to observe very small changes of electric polarization (Fig. 6). The curves are obtained as the result of averaging over multiple cycles, since the small pyrocurrent signal was not so easy to extract on the background of the parasitic drift and interference. Therefore they allow us to estimate the effect only qualitatively and to get its order of magnitude without claiming quantitative analysis. Interestingly, that the polarization $P(H)$ does not change a sign when a magnetic field direction is inverted thus showing the same behavior as was observed in crystals $BaSc_xFe_{12-x}O_{19}$ in the magnetic field at the angle of 45° to the c axis at T = 30 K [10,21].

Thus, in both investigated substituted systems $BaCo_xTi_xFe_{12-2x}O_{19}$ and $SrCo_xTi_xFe_{12-2x}O_{19}$ the electrical polarization is manifested, which is related to the conical spin structures and their reorientation in magnetic fields. The reason for the extremely low value of polarization is likely to be fairly low electrical resistivity of crystals that does not allow preliminary polarization of samples by cooling down in a sufficiently large electric field from the temperatures above than the temperature of the transi-

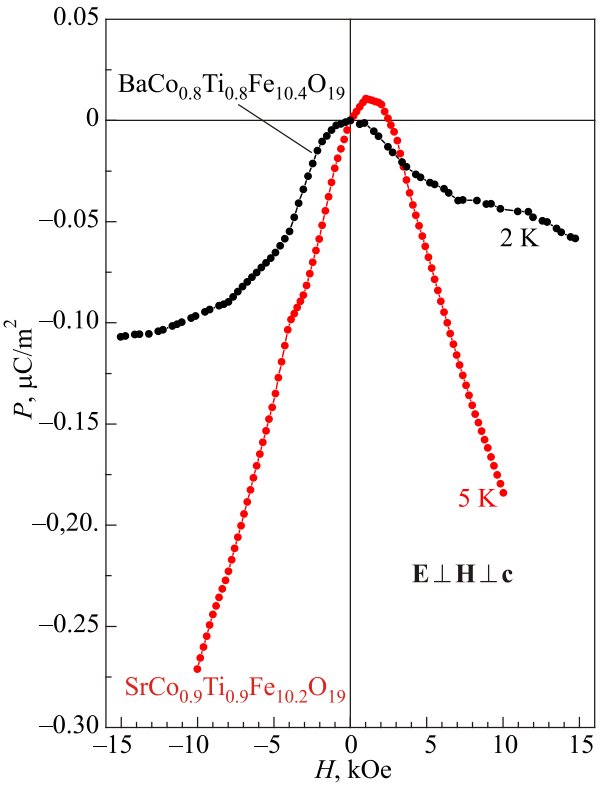

Fig. 6. The field dependences of electric polarization of the $BaCo_{0.8}Ti_{0.8}Fe_{10.4}O_{19}$ and $SrCo_{0.9}Ti_{0.9}Fe_{10.2}O_{19}$ crystals at liquid helium temperatures.

tion from the conical state to the collinear ferrimagnetic one. Our study of $Ba(Sr)Sc_xFe_{12-x}O_{19}$ [21] have shown that the value of the induced polarization is very sensitive to the magnitude of the poling electric field which decrease significantly at low values of electric fields. Two opposing factors are very important: (i) larger polarization is expected in crystals with large x and large angles of the conical structure, (ii) but they have a higher transition temperature (> 200 K for $x > 1$) that hampering a poling of a sample. On the other hand, crystals with smaller x have the lower transition temperature and can be cooled down in stronger electric fields, but a collinear ferrimagnetic structure is preserved up to the lowest temperatures and, if the conical structure still occurs, its angle remains too small resulting in a low polarization. Therefore, it is very important to increase of the electrical resistivity of the grown crystals that requires further technological developments.

4. Conclusion

Thus, as a result of the presented researches it is established:

1. High-quality single-phase hexagonal M-type barium and strontium ferrites substituted by titanium and cobalt can be obtained by floating zone melting.

2. Their magnetic properties indicate the existence of the conical spin structures at some temperatures and concentrations, which promote of magnetoelectric properties.

3. Field-induced electric polarization is observed for Ti and Co concentrations of x = 0.8–0.9. Very low value of the polarization is due to high electrical conductivity of the grown crystals which does not allow properly implement the preliminary poling of the samples and requires further improving of the technology.

The work is supported by the Russian Scientific Foundation (project 16-12-10531).

1. R.C. Pullar, *Progr. Mater. Sci*. **57**, 1191 (2012).
2. T. Kimura, G. Lawes, and A.P. Ramirez, *Phys. Rev. Lett*. **94**, 137201 (2004).
3. Y. Kitagawa, Y. Hiraoka, T. Honda, T. Ishikura, H. Nakamura, and T. Kimura, *Nature Mater*. **9**, 797 (2010).
4. M. Soda, T. Ishikura, H. Nakamura, Y. Wakabayashi, and T. Kimura, *Phys. Rev. Lett*. **106**, 087201 (2011).
5. L. Wang, D. Wang, Q. Cao, Y. Zeng, H. Xuan, J. Gao, and Y. Du, *Sci. Rep*. **223**, 1 (2012).
6. D.Y. Chen, Y.Y. Meng, D.C. Zeng , Z.W. Liu, H.Y. Yu, and X.C. Zhong, *Mater. Lett*. **76**, 84 (2012).
7. G.B. Teh, N. Saravanan, and D.A. Jefferson, *Mater. Chem. Phys*. **105**, 253 (2007)
8. V.A. Rane, S.S. Meena, S.P. Gokhale, S.M. Yusuf, G.J. Phatak, and S.K. Date, *Electr. Mat*. **42**, 761 (2013).
9. M. Mohebbi, K. Ebnabbasi, and C. Vittoria, *J. App. Phys.* **113**, 17C710 (2013),.
10. Y. Tokunaga, Y. Kaneko, D. Okuyama, S. Ishiwata, T. Arima, S. Wakimoto, K. Kakurai, Y. Taguchi, and Y. Tokura, *Phys. Rev. Lett*. **105**, 257201 (2010).
11. J. Jalli, Y.K. Hong, S.H. Gee, *S. Bae*, *J.J. Lee*, *J.C. Sur*, *G.S. Abo*, A. *Lyle*, *S.I. Lee*, H.C. *Lee*, and T. Mewes, *IEEE Trans. Magnet*. **14**, 2978 (2008).
12. D.A. Vinnik, D.A. Zherebtsov, L.S. Mashkovtseva, S. Nemrava, N.S. Perov, A.S. Semisalova, I.V. Krivtsov, L.I. Isaenko, G.G. Mikhailov, and R. Niewa, *Crystal Growth and Design* **14**, 5834 (2014).
13. N. Langhof, D. Seifert, and M. Gobbels, *J. Solid State Chem.* **182**, 2409 (2009).
14. A.M. Balbashov and S.K. Egorov, *J. Cryst. Growth* **52**, 498 (1981).
15. S. Ishiwata, Y. Taguchi, H. Murakawa, Y. Onose, and Y. Tokura, *Science* **319**, 1643 (2008).
16. H. Katsura, N. Nagaosa, and A.V. Balatsky, *Phys. Rev. Lett*. **95**, 057205 (2005).
17. I.A. Sergienko and E. Dagotto, *Phys. Rev. B* **73**, 094434 (2006).
18. R.A. Sadykov, O.P. Aleshko-Ozhevskii, and N.A. Artemiev, *Sov. Phys. Solid State* **23**, 1090 (1981).
19. J. Kreisel, H. Vincent, F. Tasset, M. Paté, and J.P. Ganne, *J. Magn. Magn. Mater*. **224**, 17 (2001).
20. X. Batlle, X. Obradors, J. Rodríguez-Carvajal, M. Pernet, V. Cabañas, and M. Vallet, *J. Appl. Phys.* **70**, 1614 (1991).
21. A.M. Balbashov, V.Yu. Ivanov, A.A. Mukhin, L.D. Iskhakova, Yu.F. Popov, G.P. Vorob'ev, and M.E. Voronchikhina, *JETP Lett*. **101**, 489 (2015).
22. M. Mihalik, V. Sirenko, A.M. Balbashov, V. Eremenko, M. Mihalik, and M. Zentkova, *Physics Procedia*, 20th Intern. Conf. Magnetism **75**, 259 (2015).
23. M. Zentkova, M. Mihalik, M. Mihalik Jr., V. Sirenko, V.V. Eremenko, A.M. Balbashov, L. Kvetkova, V. Koval, A. Vyrostkova, J. Briancin, X. Wang, and K. Kamenev, *Ferroelectrics* **499**, 1 (2016).